This article has been accepted for publication in IEEE Access. This is the author's version which has not been fully edited and content may change prior to final publication. Citation information: DOI 10.1109/ACCESS.2024.3351721

IEEE Access
Multidisciplinary | Rapid Review | Open Access Journal

Date of publication xxxx 011, 01101, date of current version x1xx 00, 0010..

Digital Object Identifier 1478510/ACCESS.2021.Doi Number

Optimal Power Flow Analysis with Renewable Energy Resource Uncertainty Using Dwarf Mongoose Optimizer: Case of ADRAR Isolated Electrical Network

SOUHIL MOUASSA[1,3], AYOOB ALATEEQ[2], ABDULLAH ALASSAF[2], RAMZAN BAYINDIR[3], IBRAHIM ALSALEH2, FRANCISCO JURADO[3], (Senior Member, IEEE)

[1]Department of Electrical Engineering, University of, Bouira, 10000 Algeria
[2]Electrical Engineering Department, College of Engineering, University of Hail, Hail 55211, Saudi Arabia
[3]Electrical-Electronics Engineering Department, Technology Faculty, Gazi University, Ankara, Turkey
[4] Department of Electrical Engineering, University of Jaén, 23700 EPS Linares, Jaén

Corresponding author: Souhil MOUASSA (e-mail: souhil.mouassa@univ-bouira.dz) or (fjurado@ujaen.es)

ABSTRACT: During the last decade, meaningful advancements have occurred in global electricity grids due to the wide integration of renewable energy resources (RES). Meanwhile, these sources play an essential role in total generation cost reduction, power loss cutting, and reduction of environmental hazards related to traditional power plants. Still, however, the optimal planning and operation of the power system in the presence RES is considered a master challenge due to the their stochastic natural and intermittency. One of the most complex and motivating issues in a power system is optimal power flow (OPF), a constrained optimization problem characterized by non-linearity and non-convexity. From these specifications, researchers competed in the past decades to find optimal solutions to stochastic OPF problems while keeping system stability. To tackle this challenge, an effective optimization algorithm which mimics on the foraging behavior of dwarf mongooses' in the nature is introduced. The introduced objective function is the total charge of the system, which includes a reserve charge for overestimation and a penalty cost for underestimating two types of PV energy–solar and wind energy. To show the robustness and efficacy of the recommended optimizer, case studies on the customized IEEE 30-bus system and a realistic power system Adrar power system DZA 26-bus (isolated grid) are undertaken. Numerical findings show that the proposed DMOA beats all previous published-results and performs better over a variety of objective functions while finding high-quality optimally viable solutions. Furthermore, the one-way analysis of variance (ANOVA) test, a statistical approach, was employed to evaluate the superiority of the proposed algorithm and to highlight a certain level of confidence to our study.

INDEX TERMS Optimal power flow, Emission, Realistic power system, Dwarf mongoose optimizer, Artificial rabbits' optimization algorithm, Wind power, Solar PV power, Uncertainty, Analysis of variance (One-way ANOVA test)

LIST OF ABBREVIATIONS

P_{loss}	Total Power Losses
VD	Voltage Deviation
δ_{ij}	The change in voltage angle between i and bus j
q_{ji}	The phase angle of term F_{ji}
V_{Gi}	Amplitude of Voltage for Generator at bus i
N_{PV}	The number of PV-bus
N_{PQ}	The number of PQ buses (Load buses)
g_k	Conductance of k^{th} branch linked into i & j
V_i, V_j	Voltage amplitude in the specified bus i or j
$\lvert Y_{ij} \rvert$	Bus admittance elements matrix
S_i^{max}	Maximum of MVA-power flow bound of branch j

This work is licensed under a Creative Commons Attribution-NonCommercial-NoDerivatives 4.0 License. For more information, see https://creativecommons.org/licenses/by-nc-nd/4

This article has been accepted for publication in IEEE Access. This is the author's version which has not been fully edited and
content may change prior to final publication. Citation information: DOI 10.1109/ACCESS.2024.3351721

$Q_{D,i}$ / $P_{D,i}$	Reactive/Real power load consumption at each bus *i*
Q_{Gi} /P_{Gi}	Reactive/Active power generation at bus *i*
$V_i^{max_i^{min}}$	The upper & lower voltage-amplitude in busbar *i*
$Q_{Gi}^{min_{Gi}^{max}}$	The min & max value of power generation at bus *i*
NB/NTL	The no. of busbar / no. of transmission lines
NLB/NG	No. of load buses/ no. of generators buses
$\lambda_V, \lambda_Q, \lambda_l$	Factors of Penalty
Q_{Gi}^{min} ,Q_{Gi}^{max}	Limits on the reactive power generators
$X_i^{max_i^{min}}$	Upper/lower limit of state variables
PV	Photovoltaic Generator
WG	Wind Generator
AHA	Artificial Hummingbird Algorithm
SMA	Slime Mold Algorithm
JS	Jellyfish Search Algorithm
GTO	Gorilla Troops Optimizer
HGS	Hunger Games Search
DMOA	Dwarf Mongoose Optimization Algorithm
ARO	Artificial Rabbits Optimization
HPS-GWO	Hybrid Particle Swarm-Gray Wolf Optimizer
TG	Traditional Generator
RES	Renewable Energy Sources
SG	Solar Generator

I. INTRODUCTION

Optimal One of the essential tools of planning and management technologies for electric power networks; is the optimal power flow (OPF), which provides high-quality electrical power at reasonable prices. In short, it is the foundation of electric grids because preserving the efficiency and economics of power systems. The main goal of OPF is to identify the best way to alter the decision variables to satisfy various physical and operational constraints imposed by the electric power grid while still optimising a chosen objective function. The most frequent objective function is lowering the total cost of production. However, other objective functions include the reduction of gas emissions, active power loss, voltage stability index (VSI), and bus voltage deviation [1].

In traditional power systems, OPF analysis primarily have been focused on the power plant fuelled by fossil fuels. However, as electricity markets have been liberalized and renewable energy sources (RES) have been integrated, the study of OPF has become more complex, leading to a significant increase in the complexity of the objective function. This intricacy emerges due to the variety of functions that take into account the inherent variability and uncertainty while framing the problem. The central aim of integrating RES generators into networks is to minimize active power losses and enhance the reliability and quality of the electrical network. Moreover, they contribute to reducing environmental pollution. [1]. Additionally, it becomes essential to determine each generator's ideal system contribution as the amount of injected RES power rises. Consequently, efficient management of energy resources could facilitate various tasks for the system's operator (SO), ultimately lowering the cost of total electricity generation.

In recent decades, the OPF problem has been resolved using several conventional optimization techniques. All optimization methods used in [2], [3], [4], and [5] are traditional optimizers. Even if several of the techniques mentioned above exhibit excellent convergence characteristics, not all of them are inherently suitable for industrial applications. Nevertheless, these techniques do possess some shortcomings, which can be outlined as follows:

1) Sensitivity to the initial starting point: These methods might exhibit comparable convergence rates towards local solutions as they do towards global solutions.
2) Limited flexibility regarding real-world systems, i.e., each solution best suits a particular issue interpretation within its appropriate limitations.
3) In addition to their inflexibility, they also struggle significantly face substantial challenges when dealing with uncertainties and stochastic problems.

Thus, understanding the disadvantages of conventional optimization approaches is crucial to developing new efficient and powerful optimization techniques. [6] Significant research in meta-heuristic algorithms has been made possible in the first ten years thanks to computational intelligence approaches and the open availability of optimization-methodologies. These optimizers can move away from local solutions and provide ones that are close to the global ones, delaying convergence. An improved version of slime mould algorithm [7], A novel sine-cosine algorithm (SCA) [8], an ameliorate equilibrium optimization technique (EO) [9]. The Harris Hawks' optimization (HHO) algorithm [10], the improved version of the Heap-based optimization algorithm (IHOA) [11], the gorilla troops optimization technique (GTOT) [12], an adaptive Gaussian TLBO approach [13], and many others are used to resolve the traditional OPF problem. While the references above are only for those, who generate thermal power. In recent years, a systems employing a mix of resources to deliver high-quality electrical energy at a cost-effective generation expense. This system uses thermal, wind, and solar generators. Integrating renewable energy sources into electricity grids offers several benefits. Firstly, it helps mitigate environmental concerns by reducing greenhouse gas emissions and air-pollution associated with fossil fuel-based power generation. Secondly, it relieves the load on transmission lines by lowering real power losses and improve voltage profiles, ensuring stability and efficient operation. The literature in the field has published a minor number of articles.

This work is licensed under a Creative Commons Attribution-NonCommercial-NoDerivatives 4.0 License. For more information, see https://creativecommons.org/licenses/by-nc-nd/4

This article has been accepted for publication in IEEE Access. This is the author's version which has not been fully edited and
content may change prior to final publication. Citation information: DOI 10.1109/ACCESS.2024.3351721

For instance, an efficient hybrid optimizer HPS-GWO is employed in [14] to solve an OPF that integrates RES while considering different objective functions to ameliorate recorded findings compared against methods. However, no forecasting method was applied to forecast wind- and PV power output. The findings indicate that MJAYA outperforms the core Jaya algorithm and surpasses other popular algorithms. Inam Ullah Khan et al. [15] proposed a GWO algorithm to handle the OPF issue in a system containing renewable energy producers. Weibull and lognormal Probability-Distribution-Functions (PDF) are utilized to forecast solar and wind energy production (PDF). It was also verified that the results were acceptable and independent variables fell within the allowable limits. Due to this, the findings indisputably show that the suggested model is adequate. Unfortunately, it was only tested on the medium-sized IEEE 30-bus test system. A developed version of the marine predator algorithm was suggested by Mohamed Farhat et., al, [16] for OPF analysis considering the uncertainty of renewable energy sources. The model is presented clearly, and the results are discussed, but only for the IEEE 30-bus system. The suggested model was not either applied to the real power grid. Mohamed Hosny et al. [17] introduce an improved version of wild horse optimizer to deal OPF problem considering RES uncertainty. The basis for the stochastic behaviour model is the PDF scheme. The results show how the hybrid technique EESWHO outperforms conventional WHO and other well-known optimizers such as, PSO, ICBO. Once more, the method wasn't tested by being used as a simple or real power system. OPF problem study in a solar-thermal power system was solved in [18] using ameliorate version of salp swarm algorithm. The proposed model's applicability to massive power systems was not studied, and the method was only tested on a modified IEEE 30-bus system. Authors in [19] suggested a Success-History based adaptive DE algorithm for OPF solutions incorporating stochastic RES. The Weibull PDF is the foundation for the proposed stochastic wind energy model. But once more, the simulation was only run on IEEE 30-bus test system.

The published results are positive and promising to consider the efforts mentioned above. Remember, however, that despite all the efforts done in this field over the past 50 years, more research is still needed. In contrast, even though many optimization techniques have successfully produced good results, they still have some restrictions and flaws in terms of their propensity to enter local optima and the difficulty of adjusting the main intrinsic components. No one can guarantee that the best solution will be found for every optimization problem, to be more precise. Applying these algorithms to real-world electric grids is also unusual. As a result, these gaps present an opportunity to propose or develop efficient algorithms capable of dealing with various OPF formulations.

The contributions in this work are described as:

1. To the authors' best knowledge, this is the 1st attempt to propose this optimizer to such a problem.
2. The DMO was applied to resolve the OPF problem by considering renewable energy resources (RERs) devoted to modified IEEE 30 and Practical Algerian isolated power system.
3. The findings are compared with other contemporary optimizers to authenticate the proficiency of the proposed DMO. The proposed method for different objective functions was observed to provide a better optimal cost than other optimizers.
4. The optimal generation of different energy resources (MERs) and less fuel consumption also play a role in environmental features and harmful emission reducing.

This study suggests the DMOA method to solve the OPF problem when RES and various objective functions are present. The proposed method is tested on the modified IEEE 30-bus test system. The penalty function (PF) is also employed here to address various stochastic OPF problem constraints. Due to its excellent randomization characteristics of DMOA, it possesses the ability to explore the entire search space effectively, ensuring to search for all optimal solutions without becoming stuck in a local optimum. Additionally, it is simple to implement and has a straightforward principle. Furthermore, the points below provide a clear explanation of the primary advantages of the suggested DMOA, which served as a motivating element in the choice of this solver.

• The dwarf mongoose's compensatory behavioural adaptation guarantees that a specific zone of the entire area is explored because no previously visited sleeping mounds are brought back, preventing DMOA from extensively exploring the search space.

• Different scout mongoose group movement patterns can ensure a healthy balance between exploration and exploitation in this algorithm.

• Various statistical analysis tests show that DMOA is ranked negatively, demonstrating that DMO is stable around the intended results and can quickly return to the best mean values.

The remain of the paper consists formulation of the problem of stochastic OPF in second Section. Section 3 gives the proposed DMO algorithm and the settings parameter. Simulation results, optimizer analysis, and results details are provided in fourth section. Section number 5 provides conclusions and future work.

This work is licensed under a Creative Commons Attribution-NonCommercial-NoDerivatives 4.0 License. For more information, see https://creativecommons.org/licenses/by-nc-nd/4

This article has been accepted for publication in IEEE Access. This is the author's version which has not been fully edited and
content may change prior to final publication. Citation information: DOI 10.1109/ACCESS.2024.3351721

2. PROBLEM FORMULATION

Solving OPF problem permit to identify the optimal values for decision variables, which involves minimizing a specific objective function while adhering to all physical and security constraints. Mathematically, the OPF problem can be expressed as follows:

$$\textit{Minimize the objective function} \quad F_{obj}(x,u) \tag{1}$$

$$\text{Subject to } g(x,u)\begin{cases} g(x,u)=0 \\ h(x,u)\le 0 \end{cases} \tag{2}$$

where $g(x,u)$ is the function related to the equilibrium state of the, $h(x,u)$ are the operational constraints of the network. x is the vector of values to be computed i.e. dependent variables and u is the vector of values to be assigned/modified by a heuristic algorithm i.e. independent variables. Dependent variables must remain within the permitted limits to achieve optimality and ensure the viability of solutions, which are crucial for the electric power system's security.

A. OBJECTIVE FUNCTIONS

Total generation cost, voltage stability index, and harmful pollution from traditional power units have been minimized in this study.

- *Traditional power plants:*

Fuel cost formula of traditional power units can be written as follows [16]:

$$C_{T0}(P_{TG}) = \sum_{i=1}^{N_{TG}} c_i P_{TGi}^2 + b_i P_{TGi} + a_i \tag{3}$$

The valve-point effect is modelled in adding a sine term to the quadratic function. This modification aims to capture the non-smooth and non-convex characteristics of generator cost curves in order reflect the practical pattern. Mathematically can be written as follows:

$$C_T(P_{TG}) = \sum_{i=1}^{N_{TG}} a_i + b_i P_{TGi} + c_i P_{TGi}^2 + \left| d_i \times \sin\left(e_i \left(P_{TG}^{\min} - P_{TG}\right)\right)\right| \tag{4}$$

Where $a_i, b_i, c_i, d_i,$and$e_i$are the cost coefficients of the i-th thermal generators producing power output P_{TGi}, N_{TG} and P_{TG}^{min} are the total number and the minimal of power output of power plants, respectively. For the usual units used here, the price and emission gas coefficients are given in [15].

Since renewable generators don't need fuel like traditional thermal power units, their cost-function evaluation meets specific standards. Direct costs for renewable generators make up the first standard. Mathematically expressed as follows:

$$Cost_{w,j}(P_{WS,j}) = g_j P_{WS,j} \tag{5}$$

$$Cost_{S,k}(P_{SS,k}) = h_k P_{SS,k} \tag{6}$$

where $g_j$and $h_k$respectively, are the coefficient of direct-cost attached with j^{th} wind generator (WG) and k^{th} solar generator (SG). $P_{WG,j}$ and $P_{SG,k}$are the scheduled power output from the same renewable generators

Given the uncertainty, there are two conceivable outcomes: If the power produced by the owner of wind and/or solar exceeds the expected values, the system operator must spin a reserve to guarantee that consumers receive uninterrupted power.

An overestimation of electric power is what is happening in this scenario. The expense incurred while committing reserve production units to meet the overestimated amount is known as reserve-cost [1]. The following math formulas are used to represent the RC for both renewable generators employed:

$$Cost_{RW,j}(P_{WG,j} - P_{Av,j}) = K_{RW,j}(P_{WG,j} - P_{WAv,j}) = K_{RW,j}\int_0^{P_{WG,j}} (p_{WG,j} - P_{W,j})\, f_W(P_{W,j})\, dp_{W,j} \tag{7}$$

$$Cost_{RS,k}(P_{SG,k} - P_{SAv,k}) = K_{RS,k}(P_{SG,k} - P_{SAv,k}) = K_{RS,k} * f_S(P_{SAv,k} < P_{SG,k}) * \left[P_{SG,k} - E(P_{SAv,k} < P_{SG,k})\right] \tag{8}$$

where $K_{RW,j}$ denotes coefficient of reserve-cost pertaining to wind power plant, $P_{WA,j}$ is the actual available-power from the same plant. $f_W(P_{W,j})$ is the Wind power PDF for j^{th} power plant where and more detail is given in [1]. $K_{RS,k}$is the coefficient of RC for k^{th} SG. $P_{SAv,k}$ is the actual available power from the same power station.

$f_S(P_{SAv,k} < P_{SG,k})$ is the probability of solar power-shortage occurrence than the scheduled power ($P_{SG,k}$), $f_s(P_{SAv,k} > P_{SG,k})$ is the expectation of SG above$P_{SG,k}$.

In contrast to overestimation, the second scenario is known as underestimating wind and PV solar power penetration. Here, actual power generation outpaces anticipated power generation, leaving excess electricity. The penalty cost for each extra quantity of power must be considered to address this problem, and the following equations state it.

$$C_{PW,j}(P_{WAv,j} - P_{WG,j}) = K_{PW,j}(P_{WAv,j} - P_{WG,j}) = K_{PW,j}\int_{P_{WG,j}}^{P_{Wr,j}} (P_{W,j} - p_{WG,j})\, f_W(P_{W,j})\, dp_{W,j} \tag{9}$$

$$C_{PS,k}(P_{SA,k} - P_{SG,k}) = K_{PS,k}(P_{SAv,k} - P_{SG,k}) = K_{PS,k} * f_S(P_{SAv,k} > P_{SG,k}) * \left[E(P_{SAv,k} > P_{SG,k}) - P_{SG,k}\right] \tag{10}$$

where $K_{PW,j}$is the penalty cost coefficient for the j-th WG, $P_{Wr,j}$is the rated output-power from the same windfarm. $K_{PS,k}$ is the coefficient of penalty-cost for k^{th} solar PV plant. $f_S(P_{SAv,k} > P_{SG,k})$is the probability of solar power surplus

This work is licensed under a Creative Commons Attribution-NonCommercial-NoDerivatives 4.0 License. For more information, see https://creativecommons.org/licenses/by-nc-nd/4

This article has been accepted for publication in IEEE Access. This is the author's version which has not been fully edited and
content may change prior to final publication. Citation information: DOI 10.1109/ACCESS.2024.3351721

i.e, actual power above the scheduled power ($P_{SG,k}$), $f_S(P_{SAv,k} > P_{SG,k})$ is the expectation of SG above $P_{ss,k}.E(P_{SAv,k} > P_{SG,k})$.

It is crucial to note that the cost assessment of wind turbines and solar photovoltaic units relies on the wind's Weibull probability distribution functions (PDF) and the sun's lognormal PDF, respectively [20].

Objective 1: All the aforementioned cost-functions are included in the 1st objective function, which is created with the existence of RES. This goal reduces the cost of generation while excluding the cost of emissions. Mathematical expressions include:

$$F_{Obj}^{1} = C_T(P_{TG}) = \sum_{j=1}^{N_{WG}} [C_{W,j}(P_{WGs,j}) + C_{RW,j}(P_{WG,j} - P_{WAv,j}) + C_{PW,j}(P_{WAv,j} - P_{WG,j})] + \sum_{k=1}^{N_{SG}} [C_{S,k}(P_{SG,k}) + C_{RS,k}(P_{SG,k} - P_{SAv,k}) + C_{PS,k}(P_{SAv,k} - P_{SG,k})] \quad (11)$$

Where N_{WG} and N_{SG} denote the number of wind generators and solar generator in the grid.

Objective 2: *Pollution and tax of carbon*

A harmful gases such as SO_X, NO_X, and CO_2, emit during the combustion process in thermal power plants. To mitigate the environmental impact of thermal generators, an efficient strategy was adopted by including the carbon tax as penalty to encourage greenhouse gas reduction responsible for climate change. This goal can be accomplished by minimising the cost of production and emissions, which is represented as:

Second objective function Minimize-

$$F_{Obj}^{2} = F_{Obj}^{1} + C_{tax} \times E \quad (12)$$

$$E = \sum_{i=1}^{N_{TG}} [(\alpha_i + \beta_i P_{TGi} + \gamma_i P_{TGi}^2) \times 0.01 + \omega_i \, exp(\mu_i P_{TGi})] \quad (13)$$

where $\alpha_i, \beta_i, \gamma_i, \omega i, \mu i$ denote the emission-factors connecting with i-th power plant & C_{tax} is the fixed tax of Carbon, equal to 20 ($/h).

Objective 3: Index of voltage stability improvement

With huge penetration of renewable energy sources to grid, power network monitoring and management have become extremely important in designing, planning, and operating modern electric power systems. To this end, index of voltage stability is minimized to achieve advance information's on the voltage drops in the network. Index L's operating range was set to [0, 1]. The voltage stability index is also minimized; its function might be written as follows:

$$F_{Obj}^{3} = \min(VSI) = min(max(L_j)) \quad (14)$$

where L_j of the j^{th} bus is written as follows:

$$L_j = \left|1 - \sum_{i=1}^{N_{PV}} F_{ji} \times \frac{V_i}{V_j} \angle\{\theta_{ji} + (\delta_i - \delta_j)\}\right| j = 1,2,..,N_{PQ} \quad (15)$$

with $$F_{ji} = |F_{ji}|\angle\theta_{ji}, V_i = |V_i|\angle\delta_i, \; V_j = |V_j|\angle\delta_j$$

$$F_{ji} = -[Y_1]^{-1} \times [Y_2] \quad (16)$$

Y_1, Y_2, Y_3, and Y_4 : denote the sub-matrices of the global matrix Y_{bus} achieved when rearranging both of load and generator buses parameters, as indicate in Eq. (17).

$$\begin{bmatrix} I_{PQ} \\ I_{PV} \end{bmatrix} = \begin{bmatrix} Y_1 & Y_2 \\ Y_3 & Y_4 \end{bmatrix} \times \begin{bmatrix} V_{PQ} \\ V_{PV} \end{bmatrix} \quad (17)$$

Where V_i, V_j are the voltage amplitude at different bus-bar i & j, respectively. G_k is the conductance of k^{th} branch linked into two buses; δ_{ij} the difference of voltage angle into two buses.

B. SYSTEM CONSTRAINTS

The power flow equations related to the equilibrium state of the grid are

$$\begin{cases} P_{Gi} - P_{di} - \sum_{j=1}^{NB} |V_i| \times |V_j| \times |Y_{ij}| \times cos \times (\theta_{ij} - \delta_i + \delta_j) = 0 \\ Q_{Gi} - Q_{di} - \sum_{j=1}^{NB} |V_i| \times |V_j| \times |Y_{ij}| \times sin \times (\theta_{ij} - \delta_i + \delta_j) = 0 \end{cases} \quad (18)$$

Each constraint of operational constraints is treated as follows:

$$P_{TGi}^{\min} \le P_{TGi} \le P_{TGi}^{\max}, \qquad i = 1,2.....N_{TG} \quad (19)$$

$$P_{wsj}^{\min} \le P_{wsj} \le P_{wsj}^{\max}, \qquad j = 1,2.....N_{WG} \quad (20)$$

$$P_{ss,k}^{\min} \le P_{ss,k} \le P_{ss,k}^{\max} \qquad k = 1,2.....N_{SG} \quad (21)$$

$$Q_{TGi}^{\min} \le Q_{TGi} \le Q_{TGi}^{\max}, \quad (22)$$

$$Q_{wsj}^{\min} \le Q_{wsj} \le Q_{wsj}^{\max}, \qquad i = 1,2.....N \quad (23)$$

$$Q_{ss,k}^{\min} \le Q_{ss,k} \le Q_{ss,k}^{\max} \qquad k \in N_{SG} \quad (24)$$

$$Q_{Ci}^{\min} \le Q_{Ci} \le Q_{Ci}^{\max} \qquad i \in N_C \quad (25)$$

$$V_{Gi}^{\min} \le V_{Gi} \le V_{Gi}^{\max}, \quad (26)$$

$$V_{Li}^{\min} \le V_{Li} \le V_{Li}^{\max} \qquad i \in NL \quad (27)$$

Eqs, (19) − (21) reflect the real power limits applied on thermal generators and renewable ones, respectively. Eqs, (22) − (25) are the reactive power capabilities of traditional generators, solar/-wind generators and compensators, respectively. Whereas Eq. (26) presents the constraints applied at the generating voltage, Eq. (27) reflects the operating range of load buses voltage. No. of PV buses is abbreviated with *NL*. The number of lines in the electrical grid is named *NTL*. The static-penalty function method was one of the earliest commonly used approaches to handle limitations. The practicality of solutions is ensured by adding a significant penalty term to the objective function to punish any violations of the constraints.

This work is licensed under a Creative Commons Attribution-NonCommercial-NoDerivatives 4.0 License. For more information, see https://creativecommons.org/licenses/by-nc-nd/4

This article has been accepted for publication in IEEE Access. This is the author's version which has not been fully edited and
content may change prior to final publication. Citation information: DOI 10.1109/ACCESS.2024.3351721

Due to the avoiding repetition, the mathematical model of the uncertainty for renewable energy generators applied herein is the same of that adopted in our paper [21]

3. DMO-BASED PROPOSED ALGORITHM

In February 2022 a recent developed approach called dwarf mongoose optimization algorithm (DMOA) has been proposed by Jeffrey O. Agushaka et. *al* [22], which simulates the behavioural and social organization of mongooses in nature. The adult dwarf mongoose measures about 47 centimetres tip to tip in average and has a mean weight of 400 grams. They living collectively in groups of up to 30 individuals in zones with abundant termite mounds, rocks, and hollow trees exploiting it for hiding, especially in Africa's semi-desert and savannah bush areas. During food foraging, all individuals in the group remains very careful, whereby warn each other from a pending danger or of any potential threat, by creating an alarm call to pay attention and having enough time to avoiding the danger and hiding. In between avoiding predators, they diet of insects, larvae, beetles, scorpions, small reptiles, eggs, lizards, and rodents. One of the most interesting characteristics of dwarf mongoose is that they have a unique compensatory behavioural adaptation, which are prey size, space utilization, group size, and food provisioning. [22] These social characteristics are employed to mimics the foraging behaviour of the dwarf mongoose.

The DMOA algorithm's optimization structural model depends on three main processes: the alpha-group setting, babysitters, and the scout-group. Each group has a specific task to accomplish by contributing into the compensatory behavioural adaptation. The optimization process starts with exploring the search space from an alpha group, looking food by determines the right path-food, the distance covered, and the sleeping mounds. Certain individuals into population leave as the babysitters and the young at the nest until the group returns back at midday or evening. Then, the babysitters are exchanged for the first to forage with the group this phase termed as exploitation phase. In the exploration phase, the dwarf mongooses don't neither keep the oldest nest nor build a novel nest for their young, but they move them from sleeping mound to another and do not return to the previously explored site. Such behavior helps to explore the whole of search space effectively while avoiding to falling into local optima.

In the DMOA, each individual represents a possible solution or candidate solution for the problem at hand, and the best-solution in each iteration is the best-obtained solution. For better understanding the optimization process of DMOA, specific stages and behaviors have been expressed by mathematical model below:

3.1 Initialization of the Mongooses phase

The phase of initialization starts with generate randomly the initial positions (solutions) of the mongooses (X) between the defined problem's upper limit (ub) and lower limit (lb) for first population as shown in Eq. (31)

$$X = \begin{bmatrix} x_{1,1} & x_{1,2} & \cdots & x_{1,d-1} & x_{1,d} \\ x_{21} & x_{22} & \cdots & x_{2d-1} & x_{2,d} \\ \vdots & \vdots & x_{i,j} & \vdots & \vdots \\ x_{n,1} & x_{n,2} & \ldots & x_{n,d-1} & x_{n,d} \end{bmatrix} \begin{matrix} \rightarrow sol_1 \\ \rightarrow sol_2 \\ \rightarrow \cdots \\ \rightarrow sol_{n\times d} \end{matrix} \quad (31)$$

$$x_{i,j} = unifrnd(lower, upper, d) \quad (32)$$

where matrix X is the set of first candidate populations, which are generated randomly using Eq. (32), $x_{i,j}$ defines the location of the j^{th} dimension of the i^{th} population, n presents the Pop- size, and d is the Dimension of the problem. $unifrnd$ defines a uniformly distributed random number.

3.2 Calculating probability values involved in probabilistic selection of Alpha group

Once solutions X are obtained, their finesses are evaluated. The probability value for each population fitness is calculated by Eq. (33), and the Alpha female (α) is selected based on this probability

$$\alpha = \frac{fitn_i}{\sum_{i=1}^{n} fitn_i} \quad (33)$$

$$X_{i+1} = X_i + phi * peep \quad (34)$$

Where term $(n - bs)$ corresponds the number of mongooses in the alpha group, while bs denotes number of babysitters. $peep$ in Eq. (34) defines the vocalization of alpha female's that keeps the family into the path. phi is a uniformly distributed random number in the range $[-1,1]$, the sleeping mound (sm) after every iteration is given in Eq. (35)

$$sm_i = \frac{fit_{i+1} - fit_i}{max\{|fit_{i+1}, fit_i|\}} \quad (35)$$

To calculate average value of the sleeping mound found used Eq. (36)

$$\phi = \frac{\sum_{i=1}^{n} sm_1}{n} \quad (36)$$

After alpha group complete their searches, the algorithm shifts to the scouting stage, where the next food source or sleeping mound is evaluated once the babysitter exchange criterion is fulfilled.

3.3 Scout group phase

Since the mongooses not to return to the previous sleeping mound, the scouts seek for the next sleeping mound, which assures exploration. The scouting with foraging process is done at the same time [22]. This movement is modeled as an overall success or failure evaluation of finding a new sleeping mound. This behavior can be can be mathematically formulated as follow:

This work is licensed under a Creative Commons Attribution-NonCommercial-NoDerivatives 4.0 License. For more information, see https://creativecommons.org/licenses/by-nc-nd/4

This article has been accepted for publication in IEEE Access. This is the author's version which has not been fully edited and
content may change prior to final publication. Citation information: DOI 10.1109/ACCESS.2024.3351721

$$X_{i+1} = \begin{Bmatrix} X_i - CF * phi * rand * [X_i - \vec{M}] if \phi_{i+1} > \phi_i \\ X_i - CF * phi * rand * [X_i - \vec{M}] \quad else \end{Bmatrix} \quad \text{.....(37)}$$

Where, $CF = \left(1 - \frac{iter}{Max_{iter}}\right)^{\left(2\frac{iter}{Max_{iter}}\right)}$ defines as the parameter that command the collective-volitive movement of the mongoose group. It decreases linearly over the course of iterations.

Term M denotes the vector that redirect the mongoose to the new sleeping mound.

$$M = \sum_{i=1}^{n} \frac{X_i - sm_i}{X_i} \quad (38)$$

Figure 1 depicts the scouting group during exploration phase

3.4 The babysitters phase

The babysitters are a subset of mongooses in the group's which sponsorships the young mongooses until the mother returns from trip of food researching at midday or evening to suckle it. To reset the scouting and food source information previously fundholding by the old family members, the babysitter exchange parameter is updated. [22] The pseudocode for the proposed algorithm is presented below:



FIGURE 1. Alpha/Scouting group

TABLE 1. DMOA FOR STOCHASTIC OPF PROBLEM

DMO Algorithm

Initialize the algorithm parameters $peep$, number of search agents $nPop$and the number of babysitters bs
Set $(n - bs)$and babysitters exchange parameter L
for $iter = 1: MaxIt$

- Calculate the fitness of the individual
- Set time counter C
- Find the alpha based on Eq. 33
- Produce a candidate food position X_{i+1} using Eq. 34.
- Evaluate new fitness of X_{i+1}
- Evaluate sleeping mound by using Eq. .35.
- Compute the Average-Value of sleeping mound found using Eq. 36.
- Compute the vector of movement using Eq. 38.
- Exchange babysitters if $ifC > L$, and set
- Initialize bs position and calculate fitness $fitn \leq \alpha$
- Simulate the scout mongoose next solution (position) by using Eq. 37.
- Update best solution so far

end for
Return best solution
end

4. RESULTS AND DISCUSSIONS

4.1 TEST SYSTEM I: IEEE 30-BUS TEST NETWORK

The proposed DMOA is applied to solve specific instances of the Optimal Power Flow (OPF) problem. In order to assess the performance of the DMOA, several published or not published methods are selected for fair comparison. The modified IEEE 30-bus test system was used to investigate the suggested algorithm's potential and viability in various stochastic OPF problem-solving scenarios. Two wind generators will be added to buses #5 and #11 along with one solar generator to bus #13, as part of the modification. All data used are available in [20] and [23]. All implemented algorithms were developed and solved using the MATLAB

R2014a platform. The population size is defined at 30 people for each of the chosen scenarios, while the maximum number of iterations is specified at 200 for the Adrar power network and 300 for the IEEE 30-bus. Additionally, 30 separate runs were carried out for each example to show the consistency and robustness of DMOA, and the best solution found along with matching control variables is retained. All test-system

This work is licensed under a Creative Commons Attribution-NonCommercial-NoDerivatives 4.0 License. For more information, see https://creativecommons.org/licenses/by-nc-nd/4

This article has been accepted for publication in IEEE Access. This is the author's version which has not been fully edited and content may change prior to final publication. Citation information: DOI 10.1109/ACCESS.2024.3351721

features utilized in this work are described in Table 1. All test system control variables were treated as continuous for fairly comparison. Table 2 reports description of RES characteristics.

Table1.ELECTRIC POWER-NETWORKS CHARACTERISTICS DESCRIPTION

Data's	Realistic Power System	IEEE 30-bus [24] [25]
Number of bus	26	30
Number of generators	7+2 RES (WG+PV)	6
Number of branches	171	41
Decision variables	18	12
Case 0 for P_{Loss}, (p.u).	4.373	5.880
Case 0 of *L-index*	0.2564	0.1798
Number of population	30	
Iteration Max	$2*10^2$	$3*10^2$

Table 2. CHARACTERISTICS OF RENEWABLE GENERATORS

Wind-power generating unit			
No of turbines	Rated.power, P_{wr}(MW)	Weibull PDF parameters	
25	75	v = 7.976 m/s	$l = 9$ $p = 2$
20	60	v = 8.862 m/s	
Photovoltaic power plant			
Rated power, P_{sr} (MW)		Lognormal PDF factors	
50		M = 6 σ = 0.6	

4.2 Results of IEEE 30-bus

4.2.1 Results on case 1

The objective-function in this situation is to minimize the entire cost of generation. Results from the proposed DMOA method are based on the Weibull PDF parameters. The wind distribution and Weibull fitting from the simulation of eight thousand Monte-Carlo scenarios are shown in Figures 2-3, and Figure 4 shows the stochastic power output of a solar generator. All PDF-parameters utilized with RES are shown in Table 3.

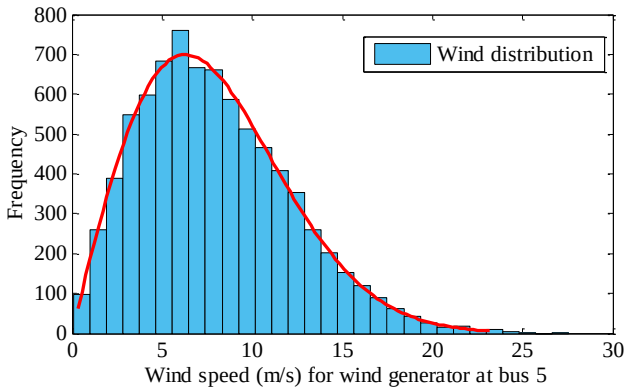


FIGURE 2. Wind speed distribution

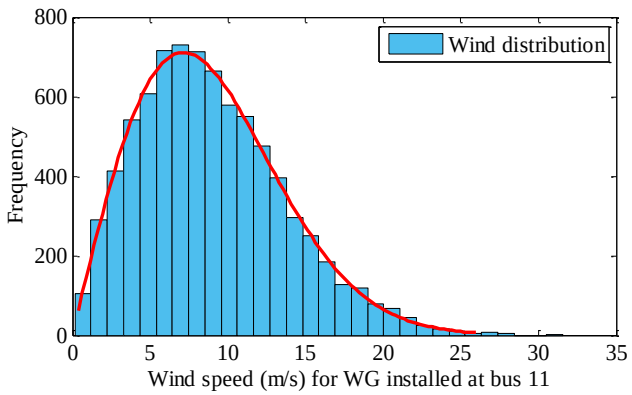


FIGURE 3. Wind speed distribution

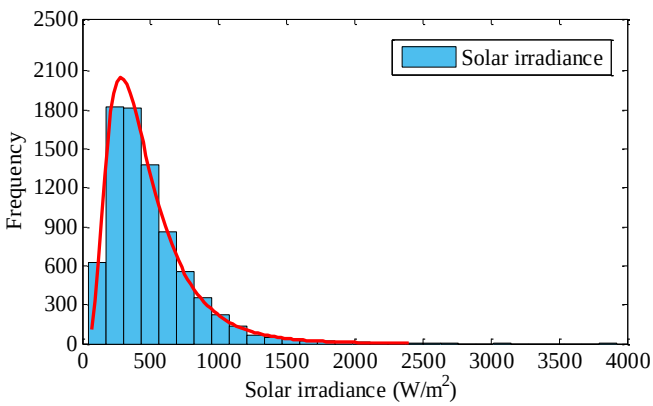


FIGURE 4. Irradiance of solar of generator installed at bus 13

This work is licensed under a Creative Commons Attribution-NonCommercial-NoDerivatives 4.0 License. For more information, see https://creativecommons.org/licenses/by-nc-nd/4

This article has been accepted for publication in IEEE Access. This is the author's version which has not been fully edited and
content may change prior to final publication. Citation information: DOI 10.1109/ACCESS.2024.3351721

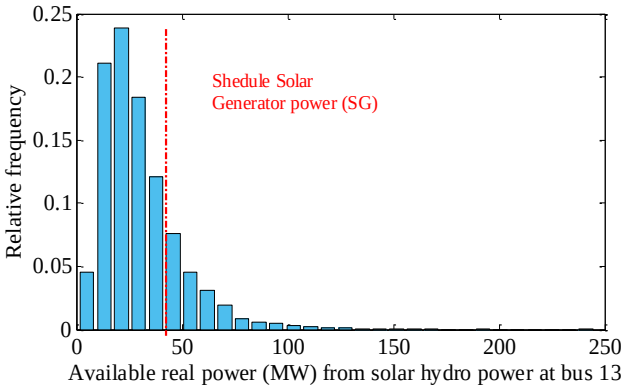


FIGURE 5. **Active power distribution of generator photovoltaic**

Table 4 presents optimal results for the objective function and optimal control variables related to case 1 that were obtained by various algorithms, including DMOA, AHA, HGS, GTO, SMA and ARO. These optimal values were within the permissible range specified in second and third columns of the same table. Figure 6 represents the convergence curve for different approaches in case 1.

The findings of case 1 reports the effectiveness of DMOA to finding a near-optimal solution, convergence speed, and quality of the solution in comparison with remaining algorithms. The better result of total cost generated by DMOAlgorithm is 780.989 MW. Hence, DMOAlgorithm surpass all contemporary either published or implemented ones in term of performance.

P_{WG1} and P_{WG2} stand for the scheduled powers from wind generators #W_{G1} and #W_{G2}, respectively. The pollution quantity is estimated based on the optimal power scheduled from traditional generators. From outcomes presented in Table 3, it can be remark that the DMOA attain up 780.989 $/h, which is the better value inside table and outperformed all other approaches, such as: MFO (781.69 $/h), SHADE-SF (782.503 $/h), JS (781.676 $/h), AHA (781.9337 $/h), HGS (781.86 $/h), slim mould algorithm (781.0786 $/h), and gorilla troops optimizer (781.262 $/h), as well as vs. a recently introduced optimizer which titled, artificial rabbits optimization ARO (781.2613 $/h).

TABLE 3. **OPTIMAL RESULTS OBTAINED FOR CASE 1 FOR DIFFERENT ALGORITHMS**

Algorith	Min	Max	MFO [20]	SHADE-SF [1]	JS [24]	AHA	HGS	GTO	SMA	ARO	DMOA
$^{*}P_{TG1}$	50	140	134.90	134.908	134. 905	134.8891	134.907	134.907	134.91	134.907	134.914
P_{TG2}	20	80	28.471	28.564	29.0226	28.3147	28.8317	28.1779	29.4961	28.1809	27.6003
P_{WG1}	0	75	44.644	43.774	43.9696	45.1640	42.8527	43.2909	42.2527	44.0866	43.1838
P_{TG3}	10	35	10.000	10	10.0006	10.0006	10.0000	10.0000	10.0034	10.0074	10.0180
P_{WG2}	0	60	36.588	36.949	37.0193	35.2396	35.3547	36.5917	37.1432	34.7753	35.8046
P_{SG1}	0	50	34.460	34.976	34.2532	35.5422	37.2989	36.1438	35.3402	37.1531	37.6001
V_1	.95	1.1	1.0798	1.072	1.07725	1.0730	1.0757	1.0725	1.0726	1.0725	1.0741
V_2	.95	1.1	1.0647	1.057	1.05698	1.0573	1.0606	1.0578	1.0590	1.0566	1.0576
V_5	.95	1.1	1.0428	1.035	1.03507	1.0359	1.0385	1.0374	1.0349	1.0342	1.0344
V_8	.95	1.1	1.1	1.04	1.03705	1.0384	1.0422	1.0395	1.0396	1.0411	1.0394
V_{11}	.95	1.1	1.1	1.1	1.0983	1.0980	1.1000	1.1000	1.1000	1.0998	1.0951
V_{13}	.95	1.1	1.0583	1.055	1.04571	1.0601	1.0582	1.0548	1.0511	1.0571	1.0531
Q_{TG1}	-20	150	-1.4418	-1.903	-0.6835	-0.13219	1.97011	-2.6423	-4.5670	-0.6065	1.67529
Q_{TG2}	-20	60	12.139	13.261	11.0011	11.5335	19.89941	12.5121	17.6960	9.6643	10.9737
Q_{WG1}	-30	35	22.405	23.181	22.6673	23.6256	26.51019	4.65643	1.98405	1.5485	2.18057
Q_{TG3}	-15	40	40.00	35.101	40.0	32.55216	39.23979	32.047	32.6825	35.360	33.3277
Q_{WG2}	-25	30	28.294	30	30	29.65492	30.000	29.7031	29.9006	29.2337	28.1558
Q_{SG}	-20	25	14.436	17.346	14.0246	19.43128	17.94308	16.09079	14.7003	16.7414	15.73256
F_{Cost} ($/h)			781.69	782.503	782.6767	781.9337	781.86	781.2626	781.0786	781.2613	780.989
VD (p.u.)`			N.R	N.R	N.R	0.47602	0.48809	0.4838	0.47015	0.4959	0.46464
PL (MW)			N.R	N.R	N.R	5.7504	5.8460	5.7117	5.7502	5.7112	5.7209
Emission (t/h)			N.R	N.R	N.R	1.76009	1.7622	1.76209	1.76215	1.7621	1.76298

P_G (MW), V (p.u.), Q_G (MVAr), N.R: means Not. Reported,

We may conclude that the addition of RES reduced the overall production-cost from 800.00 $/h as a reference cost to 780.989 $/h, or roughly 19 $/h based on the data provided in the literature concerning to the solution of the classic OPF problem and Table 3. Based on the information you provided, if the proposed optimizer DMOA can save $19 per hour of operating time, and there are 7,500 hours of

This work is licensed under a Creative Commons Attribution-NonCommercial-NoDerivatives 4.0 License. For more information, see https://creativecommons.org/licenses/by-nc-nd/4

This article has been accepted for publication in IEEE Access. This is the author's version which has not been fully edited and content may change prior to final publication. Citation information: DOI 10.1109/ACCESS.2024.3351721

operating time in a year, the potential savings per year can be calculated as follows:

Potential savings per year = Savings per hour * Operating hours per year

= $19/hour * 7,500 hours/year= $142,500 per year.

As a result, compared to the initial system structure, i.e., without inserting RES into test system, appears that the integration of renewable power plants dramatically reduces the cost of total generation.

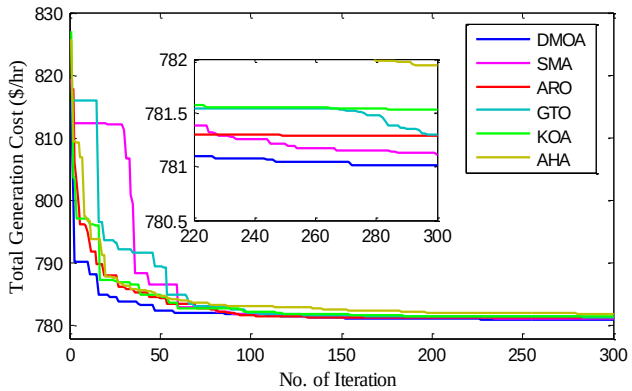


FIGURE 6. Convergence curves comparison of first case

4.2.2 Case 2: Optimization-cost versus Reserve-cost

All parameters in the second example are the same to the first case with exception of reserve cost-coefficients. These coefficients are set between 4–6 with a discrete step size of 1, i.e., = 4 for (case 2-A), = 5 for (case 2-B), = 6 for (case 2-C). This applies to both wind generators and solar photovoltaic units. All intermittent sources have penalty cost-coefficients that are comparable to the first scenario. Figure 7's bar graph displays the generators' ideal power plant, and it contrasts it with the results for the base scenario (case 1). Case 2-a describes the situation when the reserve coefficient is present. Case 2-A stands for *Kr* = 4, Case 2-B for *Kr* = 5 and Case 2-C for *Kr* = 6. In this example study, the contribution of RES decreases as the coefficient of reserve cost rises, leading to a shortage of scheduled electricity. Therefore, there is a critical requirement for spinning reserve to make up for this deficiency.

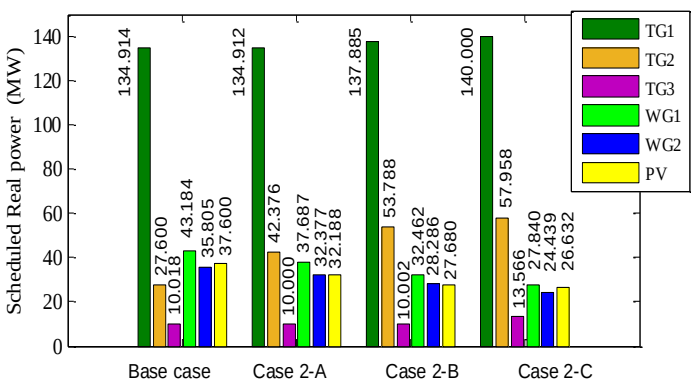


FIGURE 7. Optimal Scheduled Active Power Against Reserve Cost Coefficient (Case 2)

Thermal generators act in automatic way increasing production to fill the shortage of the contracted amount of power with grid operator. Meanwhile, as a result of the higher output power shown as seen in Figure 7, thermal power generator costs increased too. Under these circumstances, it can be concluding that the reserve-cost coefficient rises along with the total generation cost.

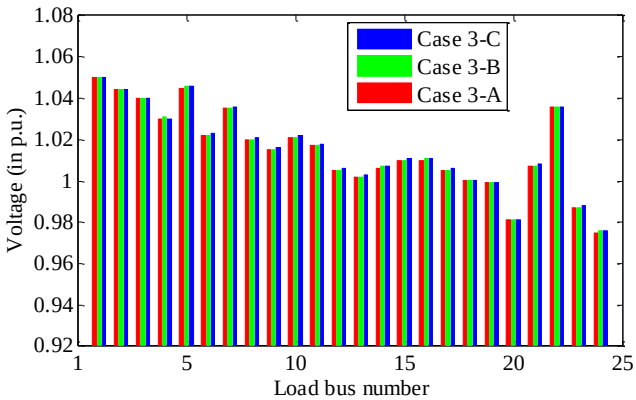


FIGURE 8. Voltage magnitudes at PV-buses

Case 3: Optimization-cost versus Penalty-cost

In contrast in the 2nd scenario, scenario, all reserve cost parameters are maintained, with the exception of the penalty cost-coefficients (PCC). The PCC for renewable generator are increased from 1.5 to 5 in this order: = 3 (Case 3-a), = 4 (Case 3-b), and = 5 (case 3-c). Bar graph of Figure 9 depicts the ideal power schedule for six generators when comparing it with results found at case 1.

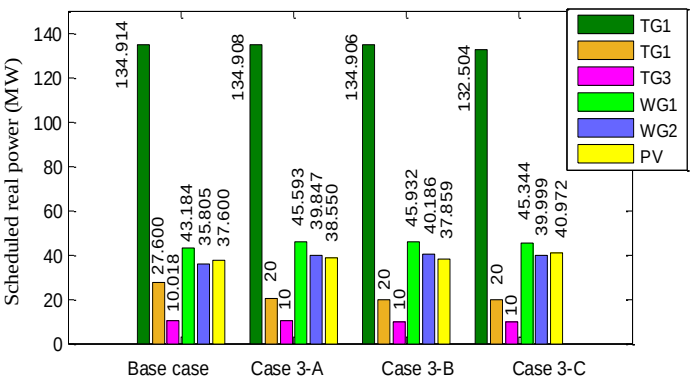


FIGURE 9. Optimal outcomes of scheduled active power when varying the penalty cost factor

As the penalty cost coefficient rises, the resulting power from renewable generators increase, which leads to fall in the output power of thermal units. The economic dispatch of power among the three thermal generators, where a sizeable

This work is licensed under a Creative Commons Attribution-NonCommercial-NoDerivatives 4.0 License. For more information, see https://creativecommons.org/licenses/by-nc-nd/4

This article has been accepted for publication in IEEE Access. This is the author's version which has not been fully edited and
content may change prior to final publication. Citation information: DOI 10.1109/ACCESS.2024.3351721

amount of the power is distributed to the generator with the lower production cost. In addition, the scheduled output from green renewable energy, which clearly appears be not uniform, is explicated with the nonlinear relationship between PDF and possible penalty/ reserve cost of RES. The cost of traditional generators (Th_{Gx}) is also constant, and the total cost is continuously increasing.

4.3 SECOND TEST SYSTEM: ADRAR'S ELECTRICAL NETWORK (AEN)

Adrar's electrical network (AEN) 26-bustrical [26] has been taken into consideration as a test system to disclose the performance of the DMOA on the real-world electrical system. The Adrar electrical network (AEN) is separate from the Algerian electricity grid and is located in the southwest of the country. It was operational in the summer of 2015 and was created to satisfy the site's local energy needs. Its peak load may reach 291.2 MW. The second system comprises of two different RES: a wind farm generates up to 10.2 megawatt and a PV generator with a capacity of 20 MW, in addition to 7 gas turbine-based power plants with a combined capacity of 425.6 megawatt. Bus number 19 is the slack bus. All test system data are accessible in [27]. There is in total of eighteen variables to optimize, involving 9 real powers and 9 voltage magnitudes. *Adrar*, *Kaberten*, and *Timimoun's* 30 kV/220 kV sub-stations are fed by the wind farm at this location, which has been put up with Gamesa G52-0.850 MW turbines as convenient units. Overall characteristics are: Rated power, P_{wr} = 850 kW, twelves wind turbines (0.85×12 WT $= 10200$ kW), the cut-in, rated and cut-out wind speeds values are v_{in}= 4 m/s, v_r = 13 m/s, and v_{out}= 24 m/s. A simplified representation of isolated electrical system is depicted in Figure 10. c = 7.2 and k = 2.1 define scale & shape factors of Adrar region, respectively [27]. Further details are found in [28], [29][26]

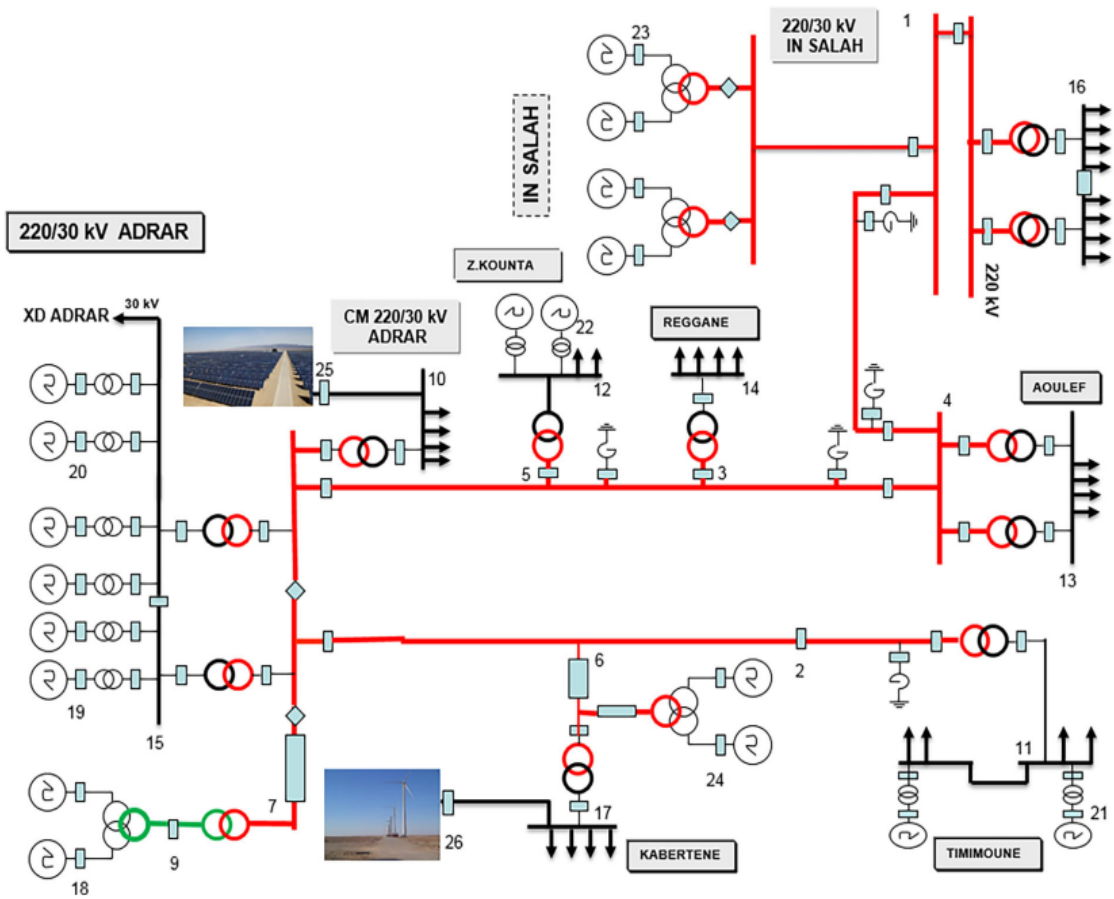


FIGURE 10. A simplified representation of isolated electrical system

The following are the wind characteristics in the Adrar region: The best wind-energy possible in Algeria for the entire 12 months is found in this zone (Adrar area), which has a mean wind speed of 7 m/s for 10-meter height. [29] [27]. In this study, four optimization techniques were applied to resolve problem at hand which is the solution of stochastic OPF problem. With the real power system, two cases are

This work is licensed under a Creative Commons Attribution-NonCommercial-NoDerivatives 4.0 License. For more information, see https://creativecommons.org/licenses/by-nc-nd/4

This article has been accepted for publication in IEEE Access. This is the author's version which has not been fully edited and
content may change prior to final publication. Citation information: DOI 10.1109/ACCESS.2024.3351721

performed: Case 1 is focused on minimize the total generating cost as given in Eq., 12; minimizing voltage stability index (VSI) is described in case 2 as indicating in equation (14).

4.3.1 RESULTS OF REALISTIC POWER SYSTEM

Table 4 reports the best outcomes achieved by DMOA algorithm and other approaches. The results unmistakably demonstrate that, when compared to existing algorithms, the DMOA offers high-quality and stable solutions. Furthermore, it can be seen that overall generation cost was greatly decreased throughout setting control variables to their optimal values. It's also it's worth noting that all various physical and operational constraints imposed by operator system are satisfied, ensuring the feasible of solutions. Also we can again notice that the total cost has significantly decreased when compared to the base case. This reduction is as a result of the addition of renewable energy sources, as we previously said.

TABLE 4. RESULTS OF THE SUGGESTED AHA, SMA, ARO, HGS, GTO, DMOA APPROACHES FOR SECOND TEST SYSTEM

	Min	Max	DMOA -	AHA	SMA	ARO	HGS	GTO	DMOA
P_{TG18}	10	24	24.00	23.203	24.00	23.4853	24.00	24.00	23.9945
$^{*}P_{TG19}$	30	220	48.9439	37.7711	35.9122	35.9867	35.8083	35.8066	35.672
P_{TG20}	4	13.6	13.6000	12.7895	13.5988	13.2832	13.60	13.60	13.5966
P_{TG21}	10	44	36.5405	33.1117	28.9737	31.7449	30.9043	30.9022	30.8857
P_{TG22}	10	50	49.9984	49.8901	49.9704	49.4362	50	50	50
P_{TG23}	20	100	80.7468	80.0902	80.2337	80.5103	79.5724	79.5813	79.5529
P_{TG24}	10	44	37.5951	25.9781	28.5339	26.7855	27.3394	27.3339	27.5228
P_{SG25}	0	20	-	19.9934	20.00	19.9994	20.00	20	20
P_{WG26}	0	10.2	-	10.1983	10.20	10.1999	10.20	10.20	10.20
V_{18}	0.95	1.1	1.1000	1.0907	1.0987	1.0942	1.1000	1.100	1.0985
V_{19}	0.95	1.1	1.0866	1.0961	1.0889	1.0873	1.0881	1.0871	1.0889
V_{20}	0.95	1.1	1.0791	1.0648	1.0770	1.0407	1.0714	1.0750	1.0739
V_{21}	0.95	1.1	1.0765	1.0742	1.0771	1.0548	1.0741	1.0740	1.0744
V_{22}	0.95	1.1	1.0905	1.0850	1.0831	1.0658	1.0904	1.0907	1.0903
V_{23}	0.95	1.1	1.0963	1.0831	1.0991	1.0849	1.0943	1.0947	1.0929
V_{24}	0.95	1.1	1.0850	1.0748	1.0727	1.0496	1.0857	1.0839	1.0809
V_{SG25}	0.95	1.1	-	1.0237	0.9597	1.0757	0.95	1.100	0.9639
V_{SG26}	0.95	1.1	-	1.0153	1.0738	0.9752	0.95	0.9604	0.9818
Q_{TG18}	-18	42	31.6345	30.5417	31.5240	48.0375	33.5441	32.2724	31.82329
Q_{TG19}	-54	126	9.5361	15.3346	11.10794	17.26794	10.3414	9.8110	10.82345
Q_{TG20}	-16	8	7.54925	1.7672	7.1049	-10.3981	1.5353	4.2133	4.21097
Q_{TG21}	-18	42	7.42534	8.7388	8.4497	8.0485	6.4176	6.3867	6.94786
Q_{TG22}	-18	42	18.9870	19.6358	17.1642	17.8426	19.2085	19.1444	19.36559
Q_{TG23}	-36	84	21.15259	20.5350	21.9041	23.9732	20.5993	20.5703	20.49642
Q_{TG24}	-16	42	12.32934	9.5603	6.9718	5.36793	12.3534	11.4188	10.41581
Q_{SG25}	-8	10	-	0.00	0.00	0.00	0.00	0.00	0.00
Q_{WG26}	-5.1	5.1	-	0.00	0.00	0.00	0.00	0.00	0.00
Fuel Cost (US$/hr)			9129.8392	8284.7188	8284.293	8284.735	8284.164	8284.129	**8283.942**
VD (p.u.)`			0.97798	0.8530	0.9442	0.6052	0.9623	0.9682	**0.95059**
PL (MW)			0.2246	0.2263	0.2228	0.2313	0.2244	0.2240	**0.2247**

This work is licensed under a Creative Commons Attribution-NonCommercial-NoDerivatives 4.0 License. For more information, see https://creativecommons.org/licenses/by-nc-nd/4

This article has been accepted for publication in IEEE Access. This is the author's version which has not been fully edited and
content may change prior to final publication. Citation information: DOI 10.1109/ACCESS.2024.3351721

NOx (kg/hr) x 1 US$/kg	**255.87**	236.50	236.30	236.45	236.04	236.05	**236.03**

P_G (MW), V (p.u.), Q_G (MVAr). $^{*}P_{TG}$: Slack-bus

The wind distribution and Weibull fitting from the simulation of 8000 Monte Carlo scenarios are displayed in Figure 11. The spotted line depicts the predetermined amount of power that the solar-PV generator is expected to supply to the grid. Figures 12 and 13 exhibit the characteristics of the probabilities of both kinds of RES. The table of results includes a list of all the control variable limits

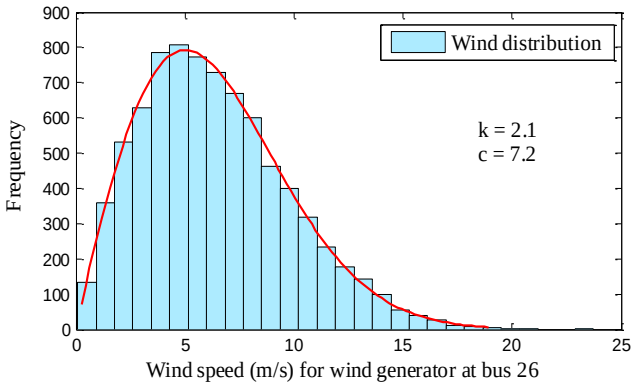


FIGURE 11. Distribution of wind speed for WG installed at bus #5

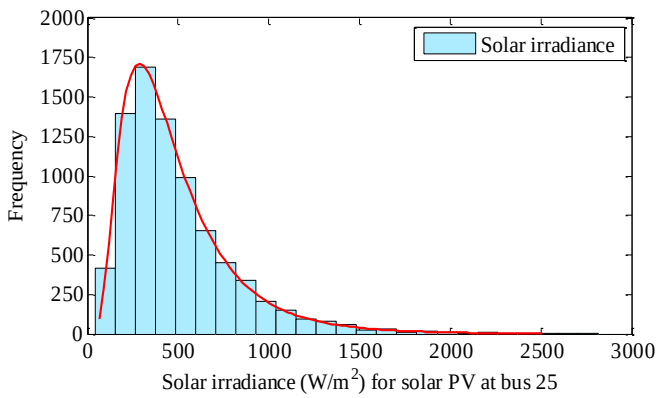


FIGURE 12. Distribution of solar irradiance or solar PV generator at bus #25

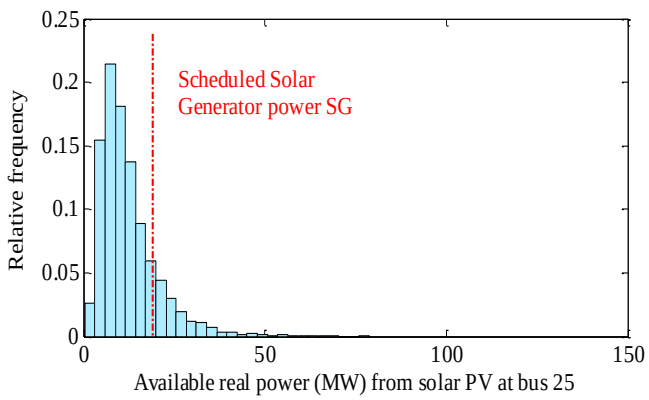


FIGURE 13. Active-power distribution (MW) of SG at bus #25

Figure 15 compares the convergence characteristics of several solutions. It is evident from a comparison of Table 4's results (DMOA-Base Case) and DMOA with RES that adding RES to the grid significantly lowers the total generating cost. Additionally, the rate of pollution amount decreased to 236 kg/hr, compared to the initial case which equal to 236 kg/hr. So, a decrease of up to 20 kg per hour, and there are 5500 hours in a year, then the pollution rate can be reduced by up to 150 tons annually. Hence, the hybrid generation system plays an important role in minimizing total cost, contributing significantly to lower atmospheric pollution and, in turn, boosting performance of the electric power grid. From a reference cost of 9129.83 US dollars per hour, overall cost of manufacturing dropped to 8283.942 (US dollars per hour), or about 845 US dollars per hour, or

up to 4.62 million US dollars per year. The simulation for the base case makes no mention of RES. A list of the outcomes from this case study's attempt to reduce total generation costs can be found in the first column of Table 4.

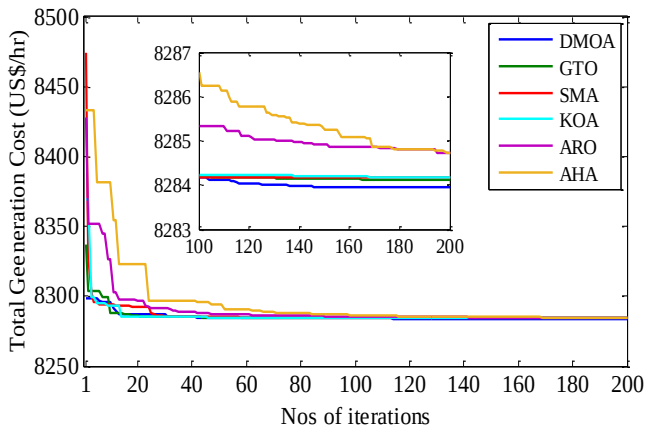


Figure 14. Convergence curves comparison of used methods

4.3.2 Outcomes of second case of realistic power network

The VSI provided by equation (14) is minimal in this situation. The P_{Loss}, VD, and NOX emissions along with the best control variables discovered using various techniques are displayed in Table 5. The outcomes unequivocally show that with regard to VSI improvement and solution convergence, the suggested DMOA performed better than all other used optimizers. It is clear from the numerical findings that all constraints variables fall within allowable bounds, indicating the viability of solutions. Voltage

This work is licensed under a Creative Commons Attribution-NonCommercial-NoDerivatives 4.0 License. For more information, see https://creativecommons.org/licenses/by-nc-nd/4

This article has been accepted for publication in IEEE Access. This is the author's version which has not been fully edited and
content may change prior to final publication. Citation information: DOI 10.1109/ACCESS.2024.3351721

magnitudes at PV buses for case 2 of Adrar's test equipment is given in Fig. 16. VSI were decreased 17.56% from the basic case. Consequently, the DMOA algorithm provides the best modification of control variables and successfully converges to near-optimal solutions, even with the practical power system. In other words, it has been demonstrated that the suggested DMOA is better suited to solve stochastic OPF compared to other solvers since it can assure the viability of outcomes found in different test power networks furthermore to benefiting from the best answers.

Table 5. OPTIMAL RESULTS OF ADRAR'S ELECTRICAL NETWORK; CASE 2

	Min	Max	AHA	SMA	ARO	HGS	GTO	DMOA
P_{TG18}	10	24	17.7942	18.4462	21.5470	20.9327	21.0308	22.9026
$^{*}P_{TG19}$	30	220	64.7148	86.3359	67.7936	59.8538	54.8319	57.8453
P_{TG20}	4	13.6	9.9768	4.8901	10.6136	13.60	13.60	13.5422
P_{TG21}	10	44	34.3989	31.9191	29.0884	35.8004	44.00	33.2211
P_{TG22}	10	50	49.7963	36.8829	48.5560	50.00	50.00	49.9942
P_{TG23}	20	100	57.0157	53.8387	61.4375	59.1584	58.8493	58.8737
P_{TG24}	10	44	29.9201	38.3322	25.4113	22.1768	19.2309	25.1557
P_{SG25}	0	20	19.9418	13.2302	19.9997	20	20	20
P_{WG26}	0	10.2	8.2354	8.1857	7.2339	10.20	10.20	10.1997
V_{18}	0.95	1.1	1.0988	1.100	1.100	1.100	1.100	1.100
V_{19}	0.95	1.1	1.0937	1.100	1.100	1.100	1.100	1.100
V_{20}	0.95	1.1	1.0850	1.0844	1.0876	1.0878	1.0879	1.0879
V_{21}	0.95	1.1	1.0968	1.0839	1.0999	1.100	1.100	1.100
V_{22}	0.95	1.1	1.0994	1.100	1.100	1.100	1.100	1.100
V_{23}	0.95	1.1	1.0985	1.100	1.0999	1.100	1.100	1.100
V_{24}	0.95	1.1	1.0971	1.0956	1.100	1.100	1.100	1.100
V_{SG25}	0.95	1.1	1.043	1.043	1.046	1.046	1.046	1.100
V_{SG26}	0.95	1.1	1.073	1.070	1.076	1.076	1.076	0.95
Q_{TG18}	-18	42	24.57464	27.99437	23.60179	22.8938	22.59585	22.7324
Q_{TG19}	-54	126	8.27416	10.92259	9.79545	9.71178	9.74462	9.8133
Q_{TG20}	-16	8	7.61067	7.57468	7.96711	8.00	8.00	7.9972
Q_{TG21}	-18	42	10.21049	6.38929	10.00186	10.36648	11.0402	10.1968
Q_{TG22}	-18	42	18.96742	18.54758	18.10950	18.23043	18.2590	18.2298
Q_{TG23}	-36	84	13.03104	13.02627	13.69070	13.18074	13.1306	13.1202
Q_{TG24}	-16	42	12.04952	13.12018	11.87327	11.68040	11.6580	11.7824
Q_{SG25}	-8	10	0.00	0.00	0.00	0.00	0.00	0.00
Q_{WG26}	-5.1	5.1	0.00	0.00	0.00	0.00	0.00	0.00
VSI (%)			21.25%	21.39%	21.17%	21.13%	21.13%	**21.13**%
PL (MW)			0.5939	0.8611	0.4809	0.5267	0.5429	**0.5346**
VD (p.u.)`			1.1566	1.1223	1.2029	1.2050	1.2033	**1.2051**
Emission (kg/hr) x 1 US$/kg			2.36×10^2	2.47×10^2	2.38×10^2	2.33×10^2	$2.33. 10^2$	**2.32**$\times 10^2$

This work is licensed under a Creative Commons Attribution-NonCommercial-NoDerivatives 4.0 License. For more information, see https://creativecommons.org/licenses/by-nc-nd/4

This article has been accepted for publication in IEEE Access. This is the author's version which has not been fully edited and
content may change prior to final publication. Citation information: DOI 10.1109/ACCESS.2024.3351721

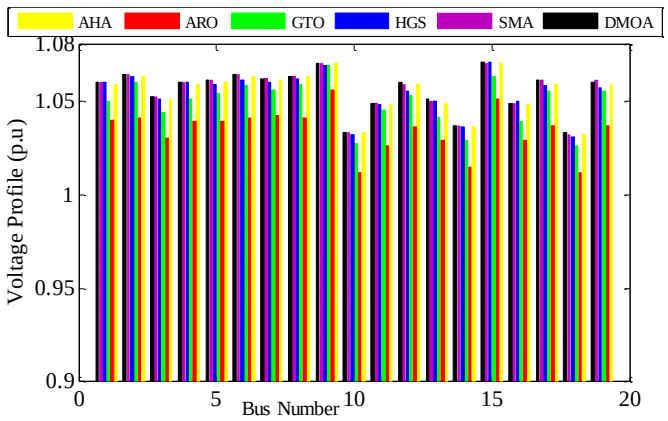


FIGURE 15. **Voltage magnitudes at load buses of second test system**

5. STATISTICAL STUDY ANALYSIS

Since the nature of stochastic algorithms, the algorithm must be executing numerous times on the same treated problem to get result values, because the results may vary from run to another. To make a fair comparison, a statistical tool based on a ANOVA test was used to check the superiority of the suggested optimizer as well as to highlight a certain level of confidence to our study. This test is necessary to assess the mean of different implemented algorithms in which there is a significant difference. In this study, the level of significance is fixed as 0.05; if P_{Value} is inferior than 5%, a significant difference between the proposed method and remaining ones happens.

Table 6a and Table 6b list the findings of one-way ANOVA on all optimizers for electric power systems where it is observed that the P-value is purely less than 5%, meaning that proposed DMOAlgorithm is statistically deferent from others algorithms.

Table 6a. Statistical results of ANOVA test, for IEEE 30 bus

Test System I: Modified-IEEE 30-bus					
variance	SS	df	MS	F	P-value
Between groups	6.0118	5	1.20236	6.49	1.476 e-5
Within groups	32.2465	174	0.18532		
Between groups	35.2583	179			

Table 6b. Statistical results of ANOVA test, for isolated network

Adrar Electrical Network					
variance	SS	df	MS	F	P-value
Between groups	26.7262	5	5.34523	55.64	2.49 e-34
Within groups	16.7163	174	0.09607		
Between groups	43.4425	179			

5. CONCLUSION

This article discusses the solution of the probabilistic OPF problem in the modern power system using a recent approach based on the dwarf mongooses' optimization technique. The Weibull and lognormal PDFs distributions have been used to simulate the uncertainty nature of the PV power-plant and wind energy sources, respectively. Five optimization approaches, including HGS, GTO, AHA, SMA, and artificial rabbits optimization (ARO), were implemented too. The standard IEEE 30-bus test system and the isolated power network DZ 26-bus in the Adrar region selected as test systems. To illustrate the superiority of the DMOAlgorithm, two scenarios were examined solving OPF issue was simulated with the integration of renewable energy resources, using the DMOA algorithm to pinpoint the optimal decision variables. It is seen that the DMOA approach realised exceptional performance in yielding the lowest cost value of 780.989 $/h for the modified IEEE 30-bus system. Also, in the real electrical network achieved the optimal cost of 8283.942 US$/h. These outcomes underscore the precision and robustness of the DMOA in efficiently tackling diverse instances of the OPF problem. The numerical output of the DMOA algorithm is compared to the results of five optimization approaches and other competing approaches. The results showed that the DMOA greatly outperformed ARO, JS, HGS, GTO, and AHA techniques in the base case and various sub-cases regardless of the constraints of the test system while providing a superior solution and guaranteeing the viability of findings.
The results indicate that both highly nonlinear issues and difficulties encountered in the actual world can be solved using the suggested DMOA technique. Statistical study was employed to confirm the consistency and effectiveness of the method. In forthcoming activity endeavours, strides will be taken to apply the DMOAlgorithm on the Practical larger-scale systems. incorporating FACTS devices and other RES including hydro generation.

ACKNOWLEDGMENT

This research has been funded by Scientific Research Deanship at University of Ha'il - Saudi Arabia through project number <<RG-23 172>>

REFERENCES

[1] Kaymaz, E., Duman, S. & Guvenc, U. Optimal power flow solution with stochastic wind power using the Lévy coyote optimization algorithm. Neural Comput & Applic 33, 6775–6804 (2021). https://doi.org/10.1007/s00521-020-05455-9

[2] Esdras Penêdo de Carvalho, Anésio dos Santos, ToFu Ma, reduced gradient method combined with augmented Lagrangian and barrier for the optimal power flow problem, Applied Mathematics and Computation, Volume 200, Issue 2, 2008, Pages 529-536, ISSN 0096-3003, https://doi.org/10.1016/j.amc.2007.11.025.

This work is licensed under a Creative Commons Attribution-NonCommercial-NoDerivatives 4.0 License. For more information, see https://creativecommons.org/licenses/by-nc-nd/4

This article has been accepted for publication in IEEE Access. This is the author's version which has not been fully edited and
content may change prior to final publication. Citation information: DOI 10.1109/ACCESS.2024.3351721

[3] J. Kyle Skolfield, Adolfo R. Escobedo, "Operations research in optimal power flow: A guide to recent and emerging methodologies and applications, European Journal of Operational Research, Volume 300, Issue 2, 2022, Pages 387-404, ISSN 0377-2217, https://doi.org/10.1016/j.ejor.2021.10.003.

[4] Sampath, L., Patil, B., Gooi, H., Maciejowski, J., & Ling, K. (2018). A trust-region based sequential linear programming approach for AC optimal power flow problems. https://doi.org/10.17863/CAM.34470.

[5] J. A. Momoh and J. Z. Zhu, "Improved interior point method for off problems," IEEE Trans. Power Syst., vol. 14, no. 3, pp. 1114–1120, 1999, doi: 10.1109/59.780938.

[6] M. Zohrul Islam, M. L. Othman, et al, "Marine predators' algorithm for solving single-objective optimal power flow," PLOS ONE., Vol. 16, no. 8, pp. 1–27, 2021, doi.org/10.1371/journal.pone.0256050.

[7] Yuanye Wei, Yongquan Zhou, Qifang Luo, Wu Deng, " Optimal reactive power dispatch using an improved slime mould algorithm" Energy Reports Vol 7 (2021), pp. 8742–8759. doi.org/10.1016/j.egyr.2021.11.138

[8] A.M. Shaheen., R. A. El-Sehiemy, H. M.Hasanien, A. R. GinidiA-F Attiaa, R. A. El Sehiemya, H. M. Hasanien, "Optimal power flow solution in power systems using a novel Sine-Cosine algorithm," Electrical Power and Energy Systems., Vol. 99, pp. 331–343, 2018, doi.org/10.1016/j.ijepes.2018.01.024.

[9] Lan Z, He Q, Jiao H, Yang L. An Improved Equilibrium Optimizer for Solving Optimal Power Flow Problem. *Sustainability*. 2022; 14(9):4992. https://doi.org/10.3390/su14094992.

[10] Diab. H, Abdelsalam M, and Abdelbary. A, "A multi-objective optimal power flow control of electrical transmission networks using intelligent metaheuristic optimization techniques," Sustainability., Vol. 13, no. 9, pp. 1–25, 2021, doi: org/10.3390/su13094979.

[11] A.M. Shaheen., R. A. El-Sehiemy, H. M.Hasanien, A. R. Ginidi, "An improved heap optimization algorithm for efficient energy management based optimal power flow model," Energy., Vol. 250, 2022, doi.org/10.1016/j.energy.2022.123795.

[12] Abdullah M. Shaheen et al., "Developed Gorilla Troops Technique for Optimal Power Flow Problem in Electrical Power Systems" Mathematics 2022, 10, 1636, MDPI doi.org/10.3390/math10101636.

[13] Alanazi, Abdulaziz, Mohana Alanazi, Zulfiqar Ali Memon, and Amir Mosavi, "Determining Optimal Power Flow Solutions Using New Adaptive Gaussian TLBO Method" *Applied Sciences* 12, no. 16: 7959, 2022. https://doi.org/10.3390/app12167959.

[14] Muhammad Riaz et *al*, an optimal power flow solution of a system Integrated with renewable sources using a hybrid optimizer, Sustainability, Vol. 13, issue 23 2021, Pages 1-12, https://doi.org/10.3390/su132313382.

[15] INAM ULLAH KHAN, NADEEM JAVAID, KELUM A. A. GAMAGE et al. "Heuristic algorithm based optimal power flow Model incorporating stochastic renewable energy sources," IEEE Access, vol. 8, no. c, pp. 148622 –148643, 2020, doi: 10.1109/ACCESS.2020.3015473.

[16] M. Farhat, S. Kamel, A. M. Atallah, B. Khan, "Developing marine predator algorithm for optimal power flow analysis considering uncertainty of renewable energy sources," Hindawi International Transactions on Electrical Energy Systems., Vol. 2022, pp. 16, 2022, doi.org/10.1155/2022/3714475.

[17] Z. Ullah, S. Wang, J. Radosavljevic, and J. Lai, "A Solution to the Optimal Power Flow Problem Considering WT and PV Generation," IEEE Access, vol. 7, no. c, pp. 46763–46772, 2019, doi: 10.1109/ACCESS.2019.2909561.

[18] Mohd Herwan Sulaiman, Zuriani Mustaff "An application of improved salp swarm algorithm for optimal power flow solution considering stochastic solar power generation" e-Prime - Advances in Electrical Engineering, Electronics and Energy, vol. 5, pp. 312–320, 2023, doi.org/10.1016/j.prime.2023.100195.

[19] Sharad Suman, Hemant Kumar Meena "Optimal power flow solution incorporating stochastic renewable energy sources for controlled emission" 2021 IEEE PES/IAS PowerAfrica, Nairobi, Kenya, 2021, doi.org/10.1109/PowerAfrica52236.2021.954323.

[20] Mouassa, S, Althobaiti, A, Jurado, F, Ghoneim, S.S.M, "Novel Design of Slim Mould Optimizer for the Solution of Optimal Power Flow Problems Incorporating Intermittent Sources: A Case Study of Algerian Electricity Grid," IEEE Access 2022, vol.10, pp. 22646–22661

[21] Mohd Herwan Sulaiman, Zuriani Mustaff and MIM Rashid, "An application of teaching–learning-based optimization for solving the optimal power flow problem with stochastic wind and solar power generators" Results in Control and Optimization, Vol. 10, pp. 087-100,2023

[22] J. O. Agushaka, A. E. Ezugwu, and L. Abualigah, "Dwarf Mongoose Optimization Algorithm," vol. 391, pp. 1–38, 2022.

[23] R. D. Zimmerman, C. E. Murillo Sánchez, and R. J. Thomas, "MATPOWER: Steady-State Operations, Planning, and Analysis Tools for Power Systems Research and Education," Power Syst. IEEE Trans., vol. 26, no. 1, pp. 12–19, 2011, doi: 10.1109/TPWRS.2010.2051168.

[24] M. Farhat, S. Kamel, A. M. Atallah, and B. Khan, "Optimal power flow solution based on jellyfish search optimization considering uncertainty of renewable energy sources," IEEE Access, vol. 9, pp. 100911–100933, 2021, doi: 10.1109/ACCESS.2021.3097006.

[25] S. Makhloufi, A. Mekhaldi, and M. Teguar, "Three powerful nature-inspired algorithms to optimize power flow in Algeria's Adrar power system," Energy, vol. 116, pp. 1117–1130, 2016, doi: 10.1016/j.energy.2016.10.064.

[26] M. Naidji and M. Boudour, "Stochastic multi-objective optimal reactive power dispatch considering load and renewable energy sources uncertainties: a case study of the Adrar isolated power system," Int. Trans. Electr. Energy Syst., vol. 30, no. 6, pp. 1–28, 2020, doi: 10.1002/2050-7038.12374.

[27] Chellali, A. Khellaf, A. Belouchrani, and R. Khanniche, "A comparison between wind speed distributions derived from the maximum entropy principle and Weibull distribution. Case of study; Six regions of Algeria," Renew. Sustain. Energy Rev., vol. 16, no. 1, pp. 379–385, 2012, doi: 10.1016/j.rser.2011.08.002.

[28] S. Diaf, G. Notton, and D. Diaf, "Technical and economic assessment of wind farm power generation at Adrar in Southern Algeria," Energy Procedia, vol. 42, pp. 53–62, 2013, doi: 10.1016/j.egypro.2013.11.005.

[29] S. Diaf and G. Notton, "Evaluation of electricity generation and energy cost of wind energy conversion systems in southern Algeria," Renew. Sustain. Energy Rev., vol. 23, pp. 379–390, 2013, doi: 10.1016/j.rser.2013.03.002.



SOUHIL MOUASSA was born in Ziama Mansouriah, Jijel City, Algeria. He received the B.S. degree in electrical engineering and the Magister's degrees from the University of Setif, Algeria, in 2009 and 2012, respectively, and the Ph.D. degree from the University of Jaén, Jaén, Spain, and Sétif 1 University in 2021. He is Associate Professor at University of BOUIRA, Algeria. He is a researcher between both universities. His primary research interests include optimal power system planning and operation, unconventional methods for power system analysis, micro-grids planning and operation, renewable energy, demand side management and smart homes. He works as an expert reviewer of IEEE ACCESS.

This work is licensed under a Creative Commons Attribution-NonCommercial-NoDerivatives 4.0 License. For more information, see https://creativecommons.org/licenses/by-nc-nd/4

This article has been accepted for publication in IEEE Access. This is the author's version which has not been fully edited and
content may change prior to final publication. Citation information: DOI 10.1109/ACCESS.2024.3351721



AYOOB ALATEEQ received the is an Assistant Professor in the Department of Electrical Engineering at University of Hail, Hail, Saudi Arabia where he has been since 2019. Dr. Alateeq received the B.S degree in electrical engineering from the University of Hail, Hail, Saudi Arabia, in 2009. From the University of Denver, he received the M.S and Ph.D in 2013 and 2018 respectively. His recent research interests include optimization in DC conversation



ABDULLAH ALASSAF received the B.S. degree in electrical engineering from the University of Hail, Hail, Saudi Arabia, in 2013, and the M.S. and Ph.D. degrees in electrical engineering from the University of South Florida, Tampa, FL, USA, in 2017 and 2021, respectively. He is currently an Assistant Professor in the Department of Electrical Engineering, University of Hail. His current research interests include power system dynamics and control.



RAMAZAN BAYINDIR (Senior Member, IEEE) received the bachelor's degree from the Department of Electrical Education, Gazi University, in 1992, and the M.Sc. and Ph.D. degrees from the Institute of Science and Technology, Gazi University, in 1998 and 2002, respectively. He worked as a Research Assistant and an Assistance Professor with the Department of Electrical Education, Gazi University. He became an Associate Professor at the Department of Electrical and Electronics Engineering, Gazi University, where he is currently working as a Professor. He served as the Vice Dean of the Faculty of Technology, the Director of the Gazi Vocational School, the Faculty of Technology, the Head of the Department of Electrical and Electronics Engineering in academic units. He is currently the Vice Rector of Gazi University. He has some key qualifications, such as education and curriculum design and development in different fields, vocational and technical education, designing, organization, and planning the international level projects, and educational and vocational training material development. He has more than 250 journal articles and conference papers within his field of work. He has also published as an author in four national and two international books. Having completed many national projects, he also took part in the project in which many European countries were participants. His main research interests include renewable energy sources, microgrids, distributed generation, smart grid applications, and industrial automation with programmable logic controllers (PLC). He served as a guest editor for the same SCI-indexed reputable journals. He also served as a reviewer for many high-ranked scientific journals. He is currently a Member of the Editorial Board of Turkish Journal of Electrical Engineering and Computer Sciences (Tübitak) and an Editor of IEEE A CCESS.



IBRAHIM ALSALEH (Member, IEEE) received the B.S. degree in electrical engineering from the University of Hail, Hail, Saudi Arabia, in 2012, the M.S. and Ph.D. degrees in electrical engineering from the University of South Florida, Tampa, FL, USA, in 2016 and 2020, respectively. He is currently an Assistant Professor in the Department of Electrical Engineering, University of Hail. His current research interests include optimization and reinforcement learning in smart power grids.



FRANCISCO JURADO (Senior Member, IEEE) was born in Linares Jaén, Spain. He received the M.Sc. and Dr.Ing. degrees from the National University of Distance Education, Madrid, Spain, in 1995 and 1999, respectively. Since 1985, he has been a Professor with the Department of Electrical Engineering, University of Jaén, Jaén. His current research interests include power systems, model-ing, and renewable energy.

This work is licensed under a Creative Commons Attribution-NonCommercial-NoDerivatives 4.0 License. For more information, see https://creativecommons.org/licenses/by-nc-nd/4